MODELING OSCILLATORY BEHAVIOR OF ESP WELLS UNDER TWO-PHASE FLOW CONDITIONS

Rinaldo Antonio de Melo Vieira
Mauricio Gargaglione Prado

Fonte: catálogo da BORETS.

ABSTRACT

The effect of free gas on the Electrical Submersible Pump (ESP) performance is well known. At a constant rotational speed and constant liquid flow rate, small amount of gas causes a mild head reduction when compared to the single phase liquid head. However, at higher gas rates, a drastic reduction in the head is observed. This critical condition, known as surging point, is a combination of liquid and gas flow rates that cause a maximum in the head performance curve. The first derivative of the head with respect to the liquid flow rate change sign as the liquid flow rate crosses the surging point. In several works on ESP two-phase flow performance, production conditions to the left of the surging region are described or reported as unstable operational conditions. This paper reviews basic concepts on stability of dynamical systems and shows through simulation that ESP oscillatory behavior may result from two-phase flow conditions. A specific drift flux computation code was developed to simulate the dynamic behavior of ESP wells producing without packer.

Keywords: Electrical Submersible Pump. Two-Phase Flow. Oscillatory Behavior. Transient Simulation.

1 INTRODUCTION

The mathematical model that describes the dynamic behavior of fluid flows is generically known as "conservation laws" and is represented by a set of Partial Differential Equations (PDE). These equations represent mathematical statements of the following laws of physics: mass conservation, Newton's second law and first law of thermodynamics.

If a system is described by a set of differential equations, an equilibrium solution may be determined by setting all derivatives with respect to time equal to zero. This equilibrium solution is also known as steady-state solution, fixed point, critical point, and equilibrium point, to name a few.

Several commercial steady-state two-phase codes are used by petroleum engineers to calculate the "equilibrium" flow rate for oil wells. This is a shortcut to obtain the "expected" steady-state solution, since the dynamics of the system are neglected. Some of the reasons why Steady-state simulators are so widely used include relatively low cost and easy to use when compared to more sophisticated transient simulators.

On the other hand, it is very important to distinguish between mathematical calculation and actual physical existence of a steady-state solution. An equilibrium solution may be obtained mathematically but physically may not exist or may never be achieved.

Taking for instance a two dimensional (2D) homogeneous linear system, represented by the following system of Ordinary Differential Equations (ODE):

$$\begin{cases} \dot{x}_1 = a_1 x_1 + a_2 x_2 \\ \dot{x}_2 = a_3 x_1 + a_4 x_2 \end{cases} \quad (1)$$

which can be written in matrix notation as

$$\dot{\mathbf{x}} = \mathbf{A}\mathbf{x} \quad (2)$$

The stability of the equilibrium solution (origin) is based on the eigenvalues of $\mathbf{A}$. It is asymptotically stable if, and only if, the eigenvalues have negative real parts [1].

A very useful graph that helps in the understanding of stability concepts is the phase portrait. This graph illustrates the relationship between solutions x_1 and x_2 as time evolves for several different initial conditions. Figure 1 shows a generic phase portrait, which represents a stable equilibrium. Each path corresponds to a different initial condition and the arrows provide a visual interpretation of the stability.

Figure 2 shows all possible phase portraits for 2D linear systems. The axes in this figure are given by:

$$\begin{cases} P = a_1 + a_4 \\ q = a_1 a_4 - a_2 a_3 \end{cases} \quad (3)$$

Figure 1 - Phase Portrait – Stable Node.

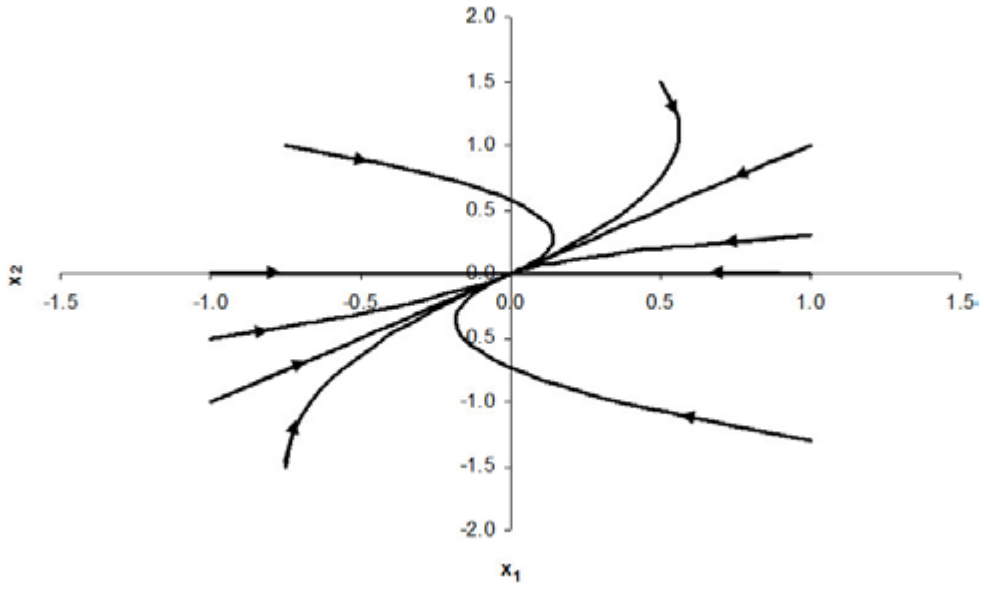

Source: AUTHOR, 2012.

Figure 2 - Equilibrium Solutions Stability – Linear 2D Problems.

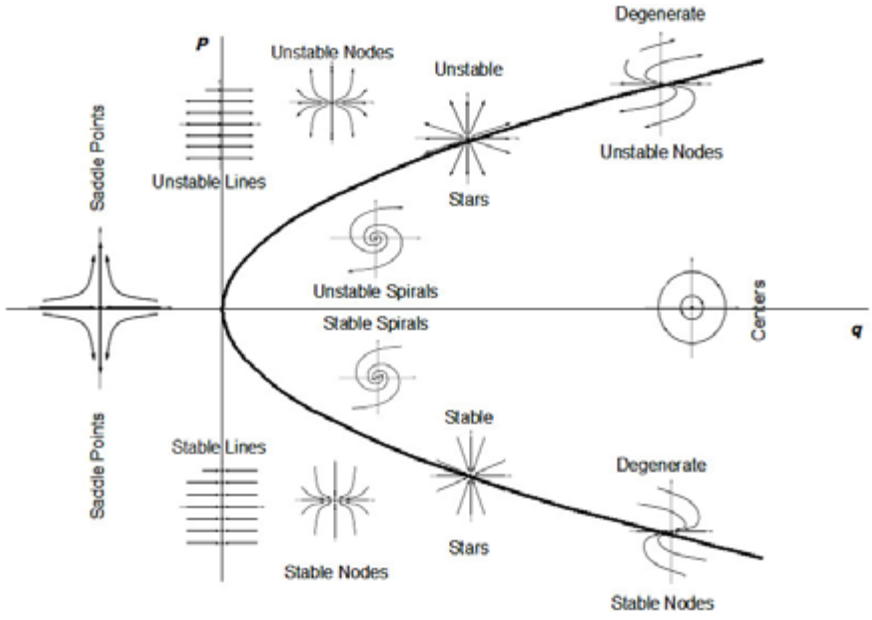

Source: AUTHOR (adapted from Wiens [2]), 2012.

The fourth quadrant of Figure 2 comprises 2D linear systems where the real part of the eigenvalues are negative, representing asymptotically stable solutions. A quick analysis of the graph reveals the presence of "neutrally stable" entities named centers. For this case, each different initial condition generates a different center which is not "attracted" nor "repelled" by the equilibrium solution. For all other situation, the paths are attracted or repelled by the equilibrium solution following lines or spirals.

The most simple and used procedure to check the stability of equilibrium solutions in nonlinear systems is known as "Local Linearization Analysis" (LLA). The linear system given by Eq. 1 can be related to the nonlinear case,

$$\begin{cases} \dot{x}_1 = f_1(x_1, x_2) \\ \dot{x}_2 = f_2(x_1, x_2) \end{cases} \tag{4}$$

where f_1 and f_2 are nonlinear functions. If small disturbances $\delta x_i(t)$ are applied to the equilibrium solutions $(\bar{x}_1, \bar{x}_2)$:

$$x_i(t) = \bar{x}_i + \delta x_i(t) \qquad i = 1, 2 \tag{5}$$

and then Equation 5 is substituted into Equation 4, the equation of how the propagation of small disturbances *around* the equilibrium solution evolves, appears. Proceeding with Taylor expansions, neglecting second and high order terms, the final linearized system is obtained. In terms of matrix notation, it is given by

$$\dot{\mathbf{x}} = \mathbf{J}\,\mathbf{x} \tag{6}$$

where $\mathbf{J}$ is the Jacobian Matrix. Similarly to the linear case, the stability of the steady-state solution *would* be given based on the eigenvalues of $\mathbf{J}$, evaluated at each equilibrium solution.

It *would* be asymptotically stable if, and only if, the eigenvalues had negative real parts. In other words, as Equation 6 represents how disturbances are propagated (in a "linearized" way), if they die-out – meaning they are attracted to the equilibrium solution – the equilibrium solution of the original non-linear system (Equation 4) is also stable and exists.

For real systems, this linearization process usually leads to easy inequalities that determine whether or not a solution is stable, which are based on steady-state parameters. Because of nonlinearities, usually these criteria are only valid in a *very small* vicinity of the equilibrium solution. In addition, another mathematical entity called "limit cycle" exists in the phase portrait of 2D nonlinear systems and is very important in determining if a steady state solution exists and if it can be achieved.

A limit cycles is an isolated closed trajectory, meaning that its neighboring trajectories are not closed – they spiral either towards (stable) or away (unstable) from the limit cycle. If one of the variables of a limit cycle is plotted against time, a periodic waveform is obtained. It only exists in nonlinear systems and cannot be determined through LLA. Transient numerical simulation is the ***only*** way to confirm the presence or not of such entity.

Figure 3 shows a very interesting situation that may occur in systems described by Equation 4. It represents a phase portrait containing a "locally" stable equilibrium solution that is surrounded by two limit cycles. The inner one is unstable while the outer, stable. The internal area of the unstable limit cycle represents the "basin of attraction" of this equilibrium solution. The equilibrium solution will only exist if the initial condition is placed inside its basin of attraction. In addition, the magnitude of any perturbation needs to be small enough to maintain the system inside this area. If these conditions are not satisfied, the limit cycle, which represents a cyclical behavior, will be the final state of the system. This example clearly shows that criteria based on LLA may be useless.

Figure 3 - Possible Phase Portrait in a 2D Nonlinear System.

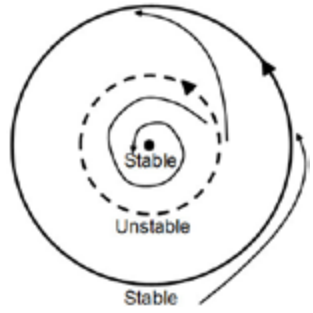

Source: AUTHOR, 2012.

3D and higher-order non-linear systems also have a different entity named "strange attractor". It represents waveforms that do not have any periodicity and remain bounded within a definite volume. This particular situation is usually called *chaos*. Figure 4 shows a well-known strange attractor named Lorenz attractor – the path never repeats itself and it remains bounded indefinitely [3].

Figure 4 - Strange Attractor [3] – Lorenz Attractor.

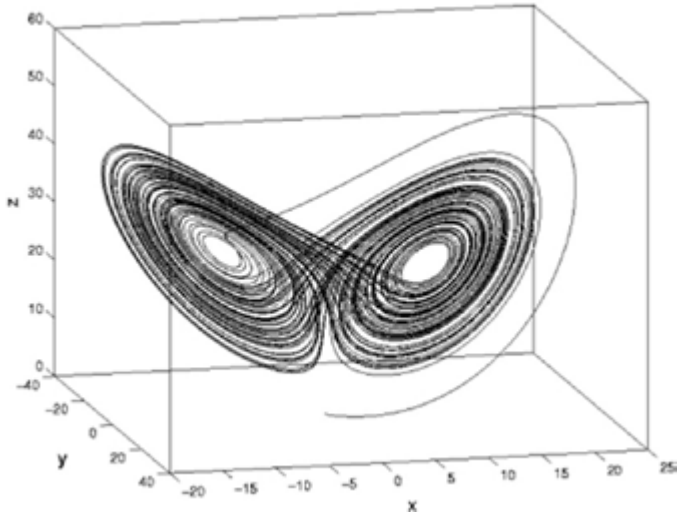

Source: COMPLEX, 2012.

Oscillatory behavior is also observed in fluid flow systems. Two phase flow system instability is a well-known problem in the nuclear industry [4, 5]. It may cause flow oscillations which can induce boiling crises, disturb control systems, or cause mechanical damage in nuclear equipment devices. Oil wells also face production instabilities that usually lead to operational problems to surface and subsurface equipment. Most importantly, they also cause production losses [6].

LLA may also be applied to fluid flow systems to determine analytical stability criteria. It is not trivial to derive such equations as the governing equations are Partial Differential Equations (PDE). To obtain easy practical criteria, several simplifying assumptions must be made. Most of them may end up reducing the system from PDE to ODE, to allow the use of LLA based on the eigenvalues of the Jacobian matrix. There exist other methods based on Laplace transformation and frequency domain but the resulting criteria are somehow equivalent. It should be noted that the number of criteria is related to the size of the Jacobian matrix.

The simplifying assumptions combined with the nonlinearities effects may cause these criteria to fail in several cases, including some very simple systems [7]. The combination of steady-state simulators and LLA criteria may not be a good choice in real case situations. Transient simulation seems to be the most adequate method to determine if a well will exhibit or not an unstable behavior.

2 TWO-PHASE FLOW MODELING OVERVIEW

2.1 THE PROBLEM BEING SOLVED

Figure 5 shows the schematic of a production well. There are basically three domains in the system: casing, tubing and annular space. One of the extremities of each domain forms a shared interface called "junction" in this work with the other domains. The casing domain comprehends the volume between the reservoir and the junction, while the tubing and the annular space are bounded by the junction and each respective surface choke.

Figure 5 - Reservoir-Casing-Tubing-Annular Space Model.

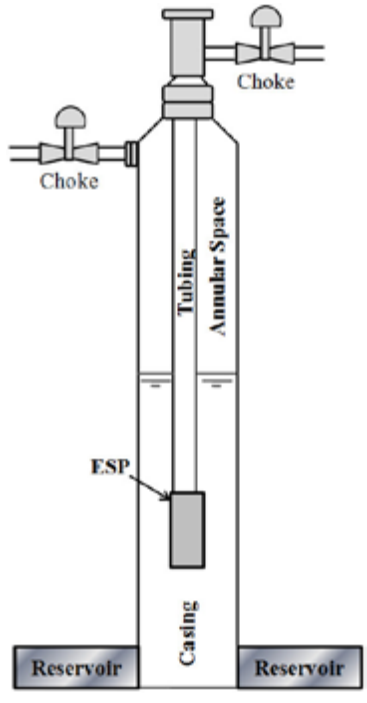

Source: AUTHOR, 2012.

Two variations are possible: (1) The ESP may be located in front of the perforations (casing not included in the solution domain) and (2) ESP in front of the perforations and the assumption that only gas is separated – all liquid from reservoir goes inside the tubing and the gas separated to the annular space vanishes (casing and annular space not included in the solution domain).

Independent of the scenario, each domain must obey the conservation laws and the junction must receive an appropriate treatment to correctly model the problem, including the consideration of gas and liquid mass conservation.

2.1.1 Equations and Numerical Solution

The model is based on the drift-flux approach [8], assuming isothermal flow and no mass transfer between phases:

$$\frac{\partial(\alpha_g \rho_g)}{\partial t} + \frac{\partial(\alpha_g \rho_g V_g)}{\partial z} = 0 \quad (7)$$

$$\frac{\partial(\alpha_l \rho_l)}{\partial t} + \frac{\partial(\alpha_l \rho_l V_l)}{\partial z} = 0 \quad (8)$$

$$\frac{\partial(\alpha_g \rho_g V_g + \alpha_l \rho_l V_l)}{\partial t} + \frac{\partial P}{\partial z} = -\rho_m g sin(\theta) + \phi_{wt} \quad (9)$$

$$V_g - V_l = V_S \quad (10)$$

where Equations 7 and 8 represent, respectively, gas and liquid mass conservation, Equation 9 the mixture momentum conservation equation (convective terms were neglected), and Equation 10 the slip velocity closure relationship.

Closure relationships must be provided for the slip velocity (V_s) and for the two-phase friction term (ϕ_{wt}). The slip velocity is obtained using the traditional drift-flux model

$$\alpha = \frac{V_{sg}}{C_0(V_{sg} + V_{sl}) + V_d} \quad (11)$$

where C_0 is the distribution parameter and V_d the drift velocity. These two parameters are obtained from published correlations. For co-current upward flow, a modification in the correlation of Woldesemayat and Ghajar [9] was proposed while for co-current downward flow Ishii and Hibiki [10] was used. Because of the lack of correlations to model counter-current flow, a linear interpolation procedure between co-current upward/downward has been developed by Vieira [7].

The discretization of the equations was done using a fully implicit first-order finite-difference method on a staggered grid [11], with pressure and void fractions defined at the cell centers and velocities at cell edges, using an upwind scheme. Equations 7-10 was discretized in each domain, with some particular adaptations such as the use of equivalent and hydraulic diameters for annular geometry.

The reservoir was modeled as a source of liquid and gas, following linear relationships. As the chokes may be under single or two-phase flow conditions, Sachdeva [12] model was used. A proper description of the "junction" was done, assuring gas and liquid mass conservation as well as pressure continuity [7].

2.1.2 Gas Separation Models

The bottomhole natural gas separation efficiency was calculated using Alhanati model [13]. This model assumes that all liquid coming from the casing goes through the pump and the liquid inside the annular space is static. These premises do not satisfy the reality of this work since the liquid within the annular space may be flowing upward or downward. Because of the lack of correlations, a modification in Alhanati's work was proposed [7].

Figure 6 shows the results of the proposed modification for some arbitrary condition. For the case when the annular liquid flow rate is zero, the correlation represents Alhanati's original model itself. If the liquid is getting into the annular space (positive flow rate) the efficiency is higher since it drags more gas. On the other hand, if the annular liquid is going inside the intake (negative flow rate) more gas is dragged into the pump, reducing the separation efficiency.

Figure 6 - Natural Casing-Annulus Separation Efficiency – Pumped Well.

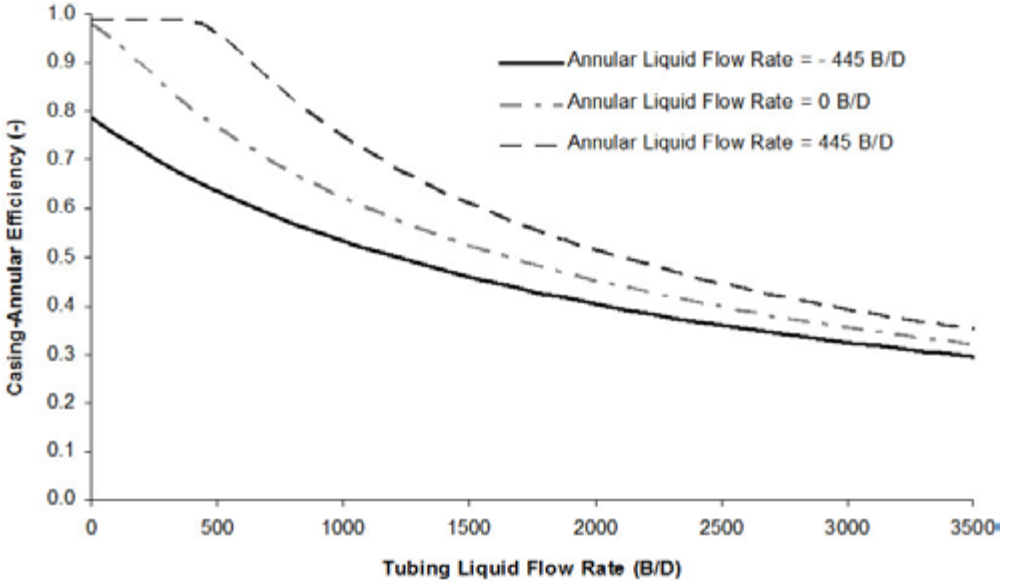

Source: AUTHOR, 2012.

A simplified rotary separator based in Alhanati's [13] rotary separator model can also be used. Figure 7 shows a typical curve for the global efficiency of this equipment, for some arbitrary conditions. As suggested by Alhanati, the existence of operational conditions in which rotary separators are not effective was considered in the simplified model.

Figure 7 - Generic Rotary Separator Efficiency Curve.

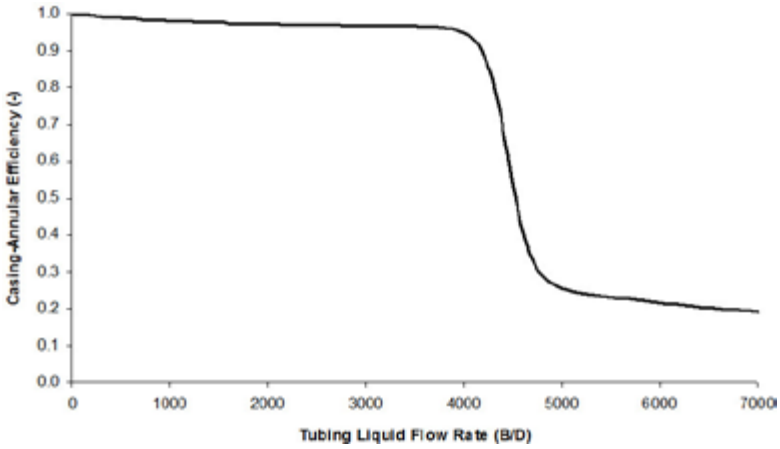

Source: AUTHOR, 2012.

2.1.3 Pump Model

Electrical Submersible Pumps are widely utilized in the oil industry. It is a multistage vertical pump with a diffuser casing that can handle large liquid volumes. In an artificial lift system, the pump is installed within a cased hole well and produces the reservoir while staying "submersed" in the fluid.

Free gas directly impacts the pump curve performance deteriorating its ability to lift liquids. The degree of head deterioration varies from a simple reduction in performance to more severe problems such as surging and gas-lock.

The pump model used in this work is proposed based on the works of Duran [14] and Carvalho [15]. The calculation is not done stage by stage; instead, it is considered an average total pressure increment. Figure 8 shows a typical curve performance for some arbitrary intake conditions for different constant gas flow rates as described by Vieira [7]. The stable operational envelope of the pump is assumed to be the region limited by the surging boundary, the water curve performance and the no-pressure increment horizontal line.

Figure 8 - Two-Phase Pump Performance Curve.

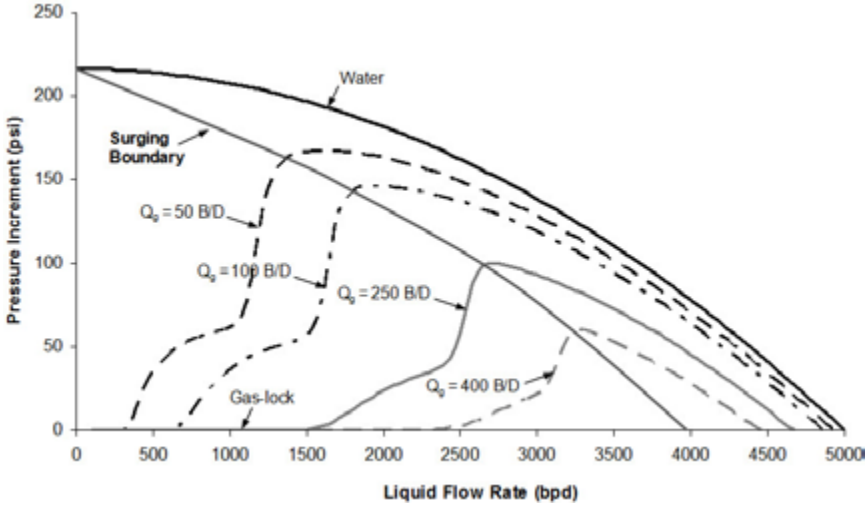

Source: AUTHOR, 2012.

3 APPLICATION AND DISCUSSION

3.1 EXAMPLE 1: NEITHER CASING NOR ANNULAR SPACE INCLUDED IN THE SOLUTION DOMAIN: UNSTABLE EXAMPLE

This example considers a pump equipped with a rotary separator. The pump maximum flow rate is 8,640 B/D and it is located in front of the perforations. The separator is under-sized as its maximum operational liquid flow rate is about 1,250 B/D. For this scenario, all liquid from reservoir goes to the pump and the gas separated to the annular space disappears.

The gas split is determined through Alhanati's model previously described. The fluids considered in this simulation are air and water. Figure 9 shows the nodal analysis under these premises.

Figure 9 - Nodal Analysis – Example 1.

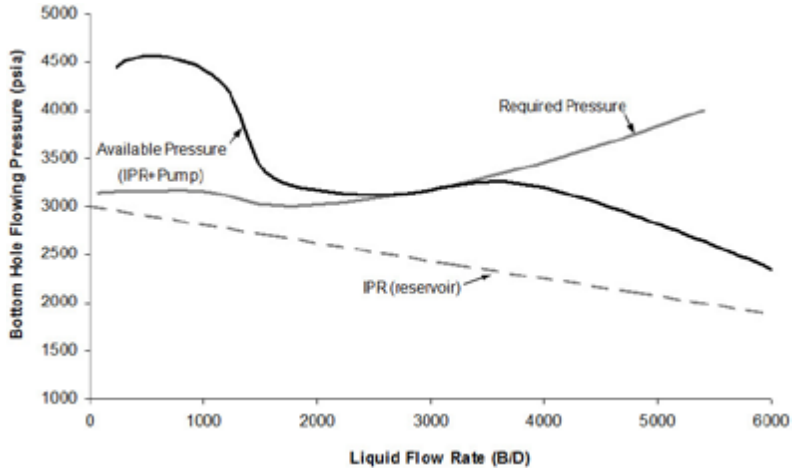

Source: AUTHOR, 2012.

One of the widely used instability criterion derived from LLA is [16]:

$$\left.\frac{dP_{avail.}}{dQ}\right|_{eq.} > \left.\frac{dP_{req.}}{dQ}\right|_{eq.} . \qquad (12)$$

According to this criterion, the solution is unstable if, at the equilibrium flow rate, the derivative of the available pressure is greater than the required pressure. Equation 12 does not guarantee that the equilibrium solution in Figure 9 is unstable. It should be noted that this is just one criterion among several others that may exist. For complex systems like this example, the other criteria are very difficult to obtain, even using simplifying assumptions.

Figure 10 shows the result of transient simulation for some initial condition. The equilibrium solution is unstable and no steady-state is obtained. The pump presents a high

frequency oscillatory behavior. An interesting observation is that the surface flow rates show small amplitudes while at the pump they are in the order of 1,500 B/D. This is not a desirable operational condition for an ESP, especially for a pump with floating impellers. In a real well, probably the protective relay would shut down the equipment.

Figure 10 - Transient Solution – Example 1 – Liquid Flow Rates.

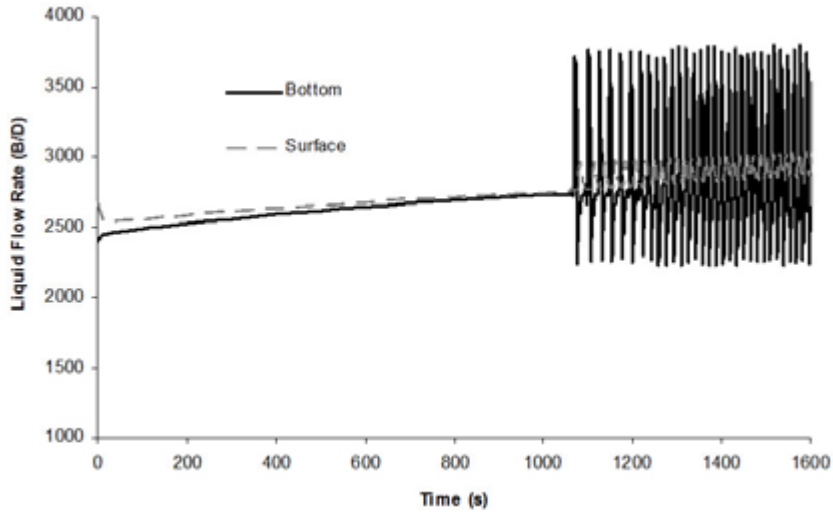

Source: AUTHOR, 2012.

3.2 EXAMPLE 2: TUBING AND ANNULAR SPACE INCLUDED IN THE SOLUTION DOMAIN: UNSTABLE EXAMPLE

The objective of this example is to determine the influence of the annular space dynamics in the unstable behavior of Example 1. To solve this problem under *steady-state conditions*, the first thing assumed is that the annular space has reached a constant dynamic level (no liquid moving inside the annular space) and thus all liquid coming from reservoir goes into the pump.

Thus, the nodal analysis is the same as the one shown in Figure 9. Figures 11 and 12 show the result of the transient simulation for some initial condition.

Figure 11 - Transient Solution – Example 2 – Tubing and Reservoir Liquid Flow Rates.

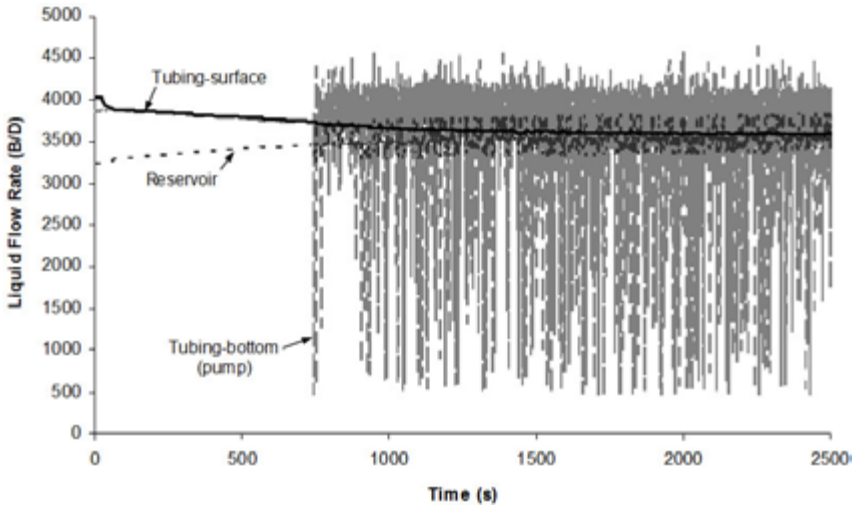

Source: AUTHOR, 2012.

The well exhibits an oscillatory behavior, confirming the previous result. It should be noted that the fluctuations at surface are even smaller while the amplitudes downhole have increased. In addition, the solution shows more evidence of a chaotic behavior.

Figure 12 - Transient Solution – Example 2 – Annular Space and Reservoir Liquid Flow Rates.

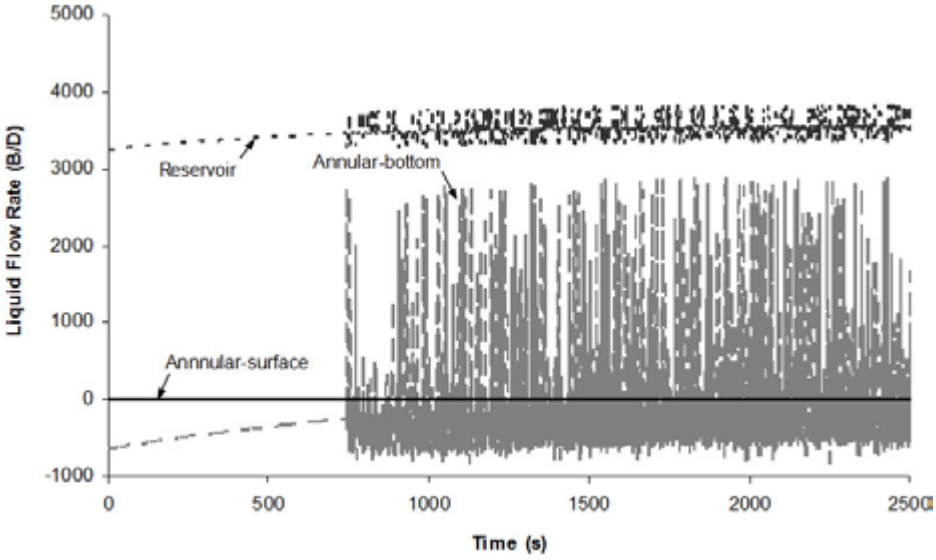

Source: AUTHOR, 2012.

3.3 EXAMPLE 3: TUBING AND ANNULAR SPACE INCLUDED IN THE SOLUTION DOMAIN: STABLE EXAMPLE

The only difference between this example and the last one is the tubing diameter. In this example, the tubing diameter is bigger than the one used in Example 2. Figure 13 shows the nodal analysis.

Figures 14 and 15 show the results of the transient simulations. The steady-state condition is reached with a constant dynamic level in the annular space, since no liquid flows in this domain after 5,000 seconds.

Figure 13 - Nodal Analysis – Example 3.

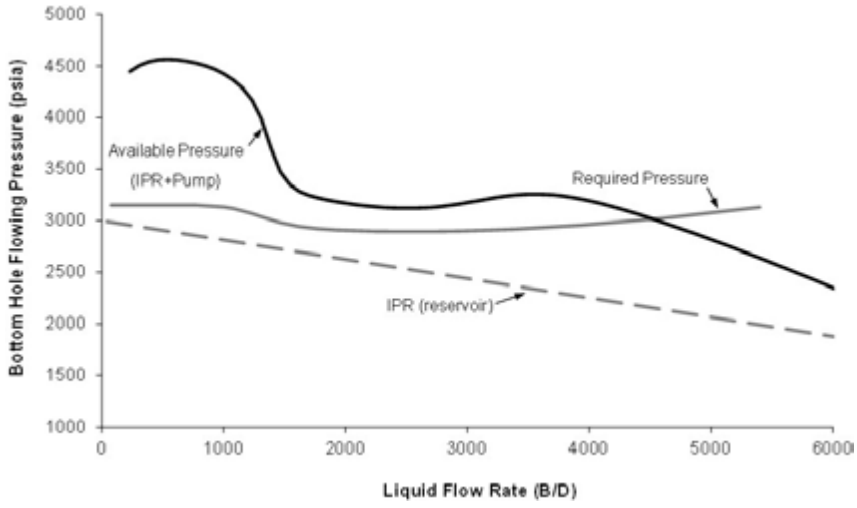

Source: AUTHOR, 2012.

Figure 14 - Transient Solution – Example 3 – Tubing and Reservoir Liquid Flow Rates.

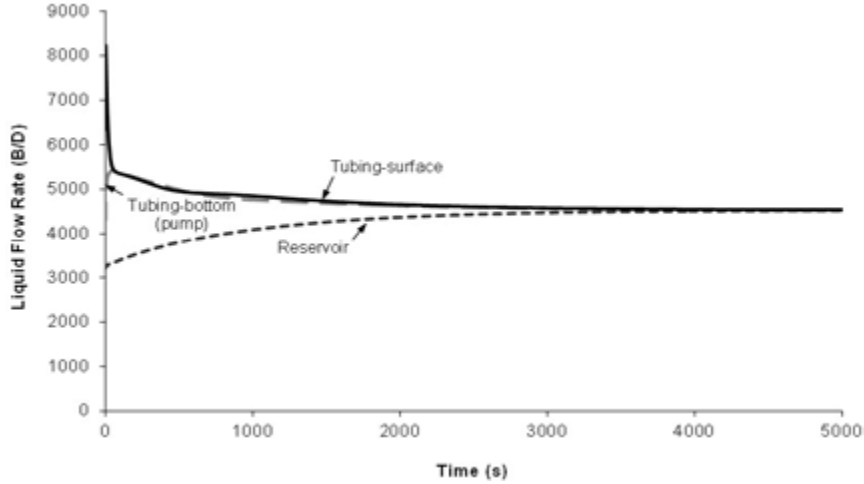

Source: AUTHOR, 2012.

Figure 15 - Transient Solution – Example 3 – Annular Space and Reservoir Liquid Flow Rates.

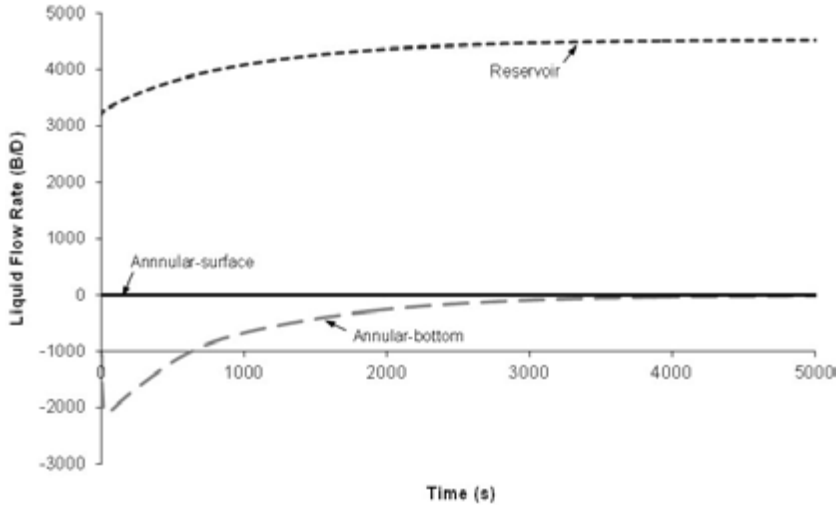

Source: AUTHOR, 2012.

It should be noted that the model developed in this work is also able to simulate the classic casing heading (natural flow wells without packers). As the objective of this work is to simulate wells equipped with ESP, no examples for this situation were shown and can be found elsewhere [7].

4 CONCLUSIONS

1. There are different attractors in multidimensional nonlinear systems, such as: equilibrium solutions, limit cycles and strange attractors. LLA provides limited information regarding a tiny piece of a big puzzle and depending on the initial condition, the equilibrium solution may never be reached, even though it is stable. Only numerical simulations can really determine whether or not a dynamic system is stable.

2. A two-phase flow code based on the drift flux approach was developed in order to simulate well configurations without packers. Under this condition, bottomhole gas segregation and storage effects were considered. For wells equipped with ESP, the two-phase flow pump performance as well as separation models were used. Due to the non-existence of models for some conditions, some modifications in similar models were proposed.

NOMENCLATURE

a_i = Constants in Matrix

$\mathbf{A}$ = Coefficient matrix

C_0 = Distribution parameter

D = Dimension

$f_i(x_1, x_2)$ = Generic nonlinear function

$\mathbf{J}$ = Jacobian Matrix

P = Pressure or trace of a 2 by 2 matrix

q = 2 by 2 matrix determinant

Q = Volumetric flow rate

t = Time

V = Velocity

V_d = Drift velocity

V_S = Slip Velocity

V_{sg} = Superficial gas velocity

V_{sl} = Superficial liquid velocity

$\dot{x}_i$ = First derivative of

$\mathbf{x}$ = Column vector of variables

$\dot{\mathbf{x}}$ = First derivative of column vector

$\bar{x}$ = Equilibrium solution

z = Position

Greek letters:

α = Gas void fraction

δ = Disturbance

θ = Angle with horizontal

ρ = Density

ϕ_{wt} = Two-phase friction loss gradient

Subscript:

avail. = Available

eq. = Equilibrium

g = Gas

l = Liquid

req. = Required

REFERENCES

[1] LOGAN, J. D. **Applied mathematics.** 3th ed. New Jersey: Wiley-Interscience, 2006. ISBN: 9780471746621.

[2] WIENS, E.G. **Two dimensional flows and phase diagrams.** Disponível em: <www.egwald.ca/nonlineardynamics/twodimensionaldynamics.php>. Acesso em: 20 dez. 2009.

[3] STROGATZ, S. H. **Nonlinear dynamics and chaos**: with applications to physics, biology, chemistry, and engineering. 1st ed. Boulder, Colorado: Westview Press, 2001.

[4] BOURE, J. A.; BERGLES, A. E.; TONG, L. S. Review of two-phase flow instabilities. **Nuclear Engineering and Design**, [S.l], v. 25, p. 165-192, 1973.

[5] LAHEY JR., R. T.; PODOWSKI, M. Z. On the analysis of various instabilities in two-phase flows. In: HEWITT, G. F.; DELHAYE, J. M.; ZUBER, N. **Multiphase science and technology.** Hemisphere, Washington, DC: Hemisphere Publishing Corp., v. 4, p. 183-370, 1989.

[6] HU, B.; GOLAN, M. **Gas-lift instability resulted production loss and its remedy by feedback control: dynamical simulation results**. In: SPE INTERNATIONAL IMPROVED OIL RECOVERY CONFERENCE IN ASIA PACIFIC, Kuala Lumpur, 2003. SPE 84917.

[7] VIEIRA, R.A.M. **Flow dynamics in oil wells.** 2011. 305 l. Thesis (Ph.D.) - University of Tulsa. Tulsa, 2011.

[8] ZUBER, N.; FINDLAY, J. A. Average volumetric concentration in two-phase flow systems. **Journal Heat Transfer,** [S.l.], v. 87, n.4, p. 453-468, 1965.

[9] WOLDESEMAYAT, M. A.; GHAJAR, A. J. Comparison of void fraction correlations for different flow patterns in horizontal and upward inclined pipes. **International Journal of Multiphase Flow.** Oxford, v. 33, n. 4, p. 347-468, Apr. 2007.

[10] ISHII, M.; HIBIKI, T. **One-Dimensional Drift-Flux Model for Various Flow Conditions.** Paper present in International Topical Meeting on Nuclear Reactor Thermal-Hydraulics, 11th. Avignon, 2005.

[11] PATANKAR, S. V. **Numerical heat transfer and fluid flow.** Washington: Hemisphere Pub. Corp.; New York: McGraw-Hill, c1980. (Series in computational methods in mechanics and thermal sciences). ISBN: 0-07-048740-5.

[12] SACHDEVA, R. **Two-phase flow through chokes.** 1984. 83 l. Thesis (M.S.E.) - University of Tulsa. Tulsa, 1984.

[13] ALHANATI, F. J. S. **Bottomhole gas separation efficiency in electrical submersible pump installations.** 1993. 140 l. Thesis (Ph.D.)- University of Tulsa. Tulsa, 1993.

[14] DURAN, J. **Pressure effects on esp stages air-water performance.** 2003. 156 l. Thesis (M.S.E.) - University of Tulsa. Tulsa, 2003.

[15] CARVALHO, P. C. G. et al. **Multiphase performance of esp stage part II**: case study. Tulsa: University of Tulsa, 2009. Technical Report.

[16] DELHAYE, J. M.; GIOT, M.; RIETHMULLER, M. L. Thermohydraulics of two-phase system for industrial design and nuclear engineering. **Chemie Ingenieur Technik**. Wahington: New York: London, v. 53, n. 12, p. 991, 1981.

[17] COMPLEX SYSTEMS LABS. Disponível em: <http://complex.upf.es/~josep/lorenzatt.jpeg>.

ACKNOWLEDGMENTS

The authors appreciate the technical and financial support of Tulsa University Artificial Lift Projects' member companies. The progress on this work is the results of the support of Baker-Hughes Centrilift, Chevron, ENI, Kuwait Oil Company, PEMEX, Petrobras, Shell International, Total and Wood Group ESP.

Rinaldo Antonio de Melo Vieira
Graduação (1999) em Engenharia Sanitária e Ambiental. Mestrado (2004) em Engenharia Química pela UFBA. Doutorado (2011) em Engenharia de Petróleo pela The University of Tulsa. Petrobras. RH/UP/ECTEP/PCPROD - Salvador, BA . Chave: CTU4.
E-mail: rinaldo_vieira@petrobras.com.br

Maurício Gargaglione Prado
Graduação (1982) em Engenharia Metalúrgia pelo IME. Mestrado (1989) em Engenharia de Petróleo pela UNICAMP. Doutorado (1995) em Engenharia de Petróleo pela The University of Tulsa. The University of Tulsa. McDougall School of Petroleum Engineering - Tulsa, OK.
E-mail: mauricio-prado@utulsa.edu